Surface Characterization Using Metastable Impact Electron Spectroscopy of Adsorbed Xenon

Y. D. Kim, J. Stultz, T. Wei, and D. W. Goodman*

Department of Chemistry, Texas A & M University, College Station, Texas 77842-3012

Received: August 21, 2002; In Final Form: October 30, 2002

In contrast to ultraviolet photoelectron spectroscopy (UPS), photoemission of adsorbed xenon (PAX) can be used for quantitative analysis of solid surfaces. In this paper, it is shown that PAX yields ambiguous results when the Xe features overlap with the substrate signals. On the other hand, with metastable impact electron spectroscopy (MIES) of adsorbed xenon (MAX), the substrate signals are completely quenched, and only the Xe features appear due to the high surface sensitivity of MIES. MAX, therefore, can provide more accurate information than PAX with respect to binding energies, energy positions, and the widths of the Xe 5p states. Several examples are given to show that MAX can be informative for the quantitative characterizations of uniform and nonuniform surfaces, illustrating that, in contrast to MIES, MAX can be used on metals as well as wide band gap materials.

1. Introduction

Ultraviolet photoelectron spectroscopy (UPS) is quite useful for the characterizations of clean and adsorbate-covered solid surfaces, however, quantifying UPS data can oftentimes be problematic. However, photoemission of adsorbed Xe (PAX) has been shown to be quantitative particularly regarding the outmost surface layer.[1,2] X-ray photoelectron spectroscopy (XPS) and Auger electron spectroscopy (AES), two other widely used techniques for quantitative surface analysis, integrate over the surface and the near-surface regions.

Metastable impact electron spectroscopy (MIES) is a non-destructive technique and extremely surface sensitive because the metastable helium atoms impinge the surface with thermal kinetic energy. Auger deexcitation (AD) is the dominant mechanism that leads to the MIES signal for wide band gap materials or metals with very low work functions. If AD is the deexcitation mechanism, a plot of the intensity of the ejected electrons versus their kinetic energies yields the surface density of states (SDOS) for the topmost layer of the surface.[3] Due to its extremely high surface sensitivity, MIES has been used to characterize subtle differences in various solid surfaces, e.g., small modifications of the surface structure that could not be detected using UPS.[4] However, for metallic and semiconductor surfaces with relatively high work functions, the yield due to the AD process is low because the dominant quenching mechanisms in these cases are resonance ionization (RI) and Auger neutralization (AN). This preference for RI and AN on these surfaces limits the application of MIES to wide band gap materials or metals with very low work functions.[3]

In this study it is shown that PAX does not give completely reliable information when superposition of the Xe peaks and the substrate features occurs. A new method, MIES of adsorbed Xe (MAX), is shown to give more accurate information with respect to binding energies, peak intensities, and full width at half-maxima (fwhm) of the Xe 5p states. This work demonstrates that MAX can be used for the characterization of surfaces for which the application of PAX is difficult due to the superposition of the Xe peaks and substrate signals. In contrast to MIES, the application of MAX is not limited to insulating materials and metals with lower work functions, but can be used on metallic surfaces with higher work function.

2. Experimental Details

The experiments were carried out in an ultrahigh vacuum (UHV) system (base pressure $= 1 \times 10^{-10}$ Torr) that consists of two interconnected chambers. One chamber was equipped with an ion gun for sputtering, low energy electron diffraction (LEED), and temperature programmed desorption (TPD). The second chamber contained AES, XPS, and MIES/UPS. MIES/UPS spectra were acquired simultaneously using a cold-cathode discharge source[5,6] that provides both ultraviolet photoelectron and metastable He 2^3S ($E^* = 19.8$ eV) atoms with thermal kinetic energy. Metastable and photon contributions to the signal were separated by a time-of-flight method using a mechanical chopper. MIES and UPS spectra were acquired with incident photon/metastable beams at 45° with respect to the surface normal using a double pass cylindrical mirror analyzer (CMA). The resolution of the analyzer, based on the width of the Fermi edge E_F is estimated to be 0.4 eV. The energy denoted by E_F in the spectra corresponds to electrons emitted from the Fermi level of the Mo substrates. In the spectra that follow, all binding energies are referenced to E_F.

The Mo(100) and Mo(112) samples were cleaned by repetitive heating to 2200 K, and the subsequent sample cleanliness confirmed using AES and LEED. A low defect MgO(100) film was prepared by Mg deposition onto Mo(100) in an O_2 environment of 1×10^{-7} Torr at 600 K, followed by multiple anneals at 1150 K. Using AES, the thickness of the MgO(100) film was determined to be approximately 15 monolayers (ML). On the bases of D_2O TPD and CO adsorption experiments, the defect density of the MgO(100) films is estimated to be minimal.[7,8]

SiO_2 thin films on Mo(112) were prepared by deposition of Si at room temperature, followed by annealing at 800 K in an

---

Surface Characterization Using MAX

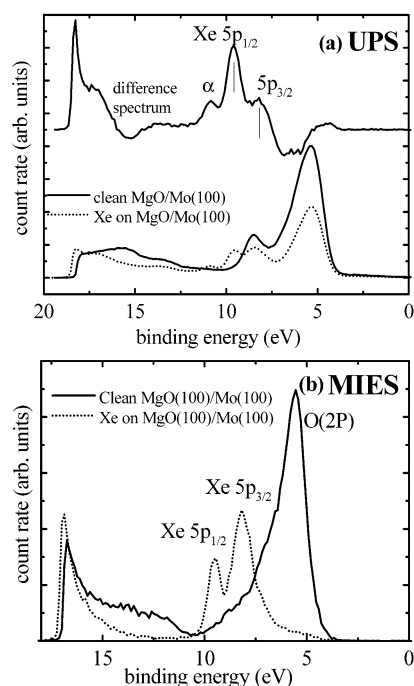*J. Phys. Chem. B, Vol. 107, No. 2, 2003* **593**

Figure 1. (a) UPS spectra for the bare and the Xe-adsorbed MgO(100)/Mo(100) surface. The difference spectrum (or the photoemission of adsorbed Xe (PAX)) is also shown. (b) MIES spectra for the bare and the Xe-adsorbed MgO(100)/Mo(100) surface. The acronym MAX is used and stands for MIES of adsorbed Xe.

O_2 environment of 1×10^{-7} Torr for 15 min. The SiO_2 films were then further annealed at 1200 K in an O_2 environment of 1×10^{-7} Torr. The AES spectra of the SiO_2 thin films showed Si^{4+} features at 78 eV, whereas no features at 90 eV due to Si^0 were observed, indicating that Si is completely oxidized to SiO_2.[9,10] For an SiO_2 thin film with a thickness of 0.7−0.8 nm, determined by the attenuation of the AES Mo peaks, LEED showed a distinct hexagonal periodicity, indicating the formation of a well-ordered SiO_2 network.[9,10]

3. Results and Discussions

3.1. MIES and UPS for Adsorbed Xe from Low Defect Surfaces. In Figure 1a, the UPS spectrum for a clean, well-ordered MgO(100) surface is compared with that of the same sample acquired in a Xe background pressure of 5×10^{-5} Torr at a sample temperature of 80 K. Under these conditions, a Xe monolayer is formed on the surface, however, multilayer formation does not.[11] Xe monolayers on solid surfaces give rise to a sharp doublet feature in UPS, originating from the $5p_{1/2}$ and $5p_{3/2}$ states of the adsorbed Xe atoms. (The $5p_{3/2}$ signal splits into two sublevels with two distinct magnetic quantum numbers, causing a broadening of the $5p_{3/2}$ peak.[12]) For MgO, the Xe-induced peaks overlap with the MgO(2P) features (Figure 1a), therefore it is necessary to subtract the normalized UPS spectrum of the clean MgO surface from that of the Xe-covered MgO surface to obtain the PAX difference spectrum at the top of Figure 1a. The difference spectrum (Figure 1a) for MgO(100) shows three features between 7 and 11 eV, two of which at lower binding energies can be assigned to the $5p_{1/2}$ and $5p_{3/2}$ states of adsorbed Xe. The third feature, α, in Figure 1a cannot be assigned. This feature does not appear if the metastable He is quenched in the MIES source chamber and only UPS spectra collected, implying that this feature might result from simultaneous interactions among Xe's, metastable He's, and UV photons. The intensities of the two Xe features and the fwhm's
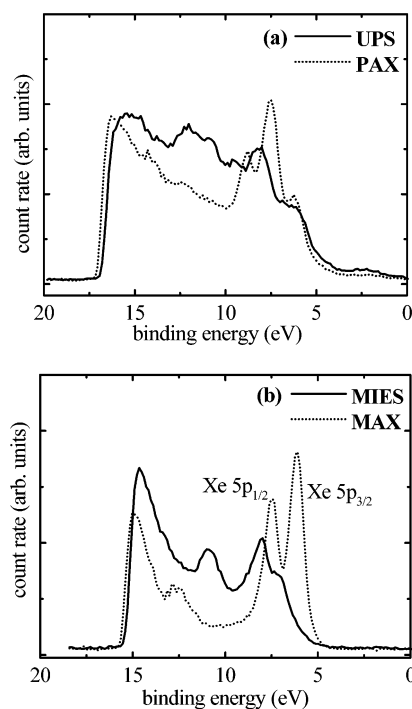
of the PAX spectra of Figure 1a are somewhat unusual in comparison with other studies;[1,2,11,13] however, it is noteworthy that difference spectra often fail to yield accurate binding energies, fwhm's, and intensities of adsorbate features.[14]

In contrast to UPS, MIES is exclusively sensitive to the surface outermost layer.[3] For example, the MIES spectrum in Figure 1b from the Xe/MgO system shows sharp peaks from the Xe 5p states. The MgO−O(2P) features are completely attenuated illustrating that MIES for adsorbed Xe can be used for the systems for which the application of the PAX is limited due to the superposition of the Xe and substrate features. The new acronym, "MAX" is used, standing for "MIES of adsorbed Xe". A higher intensity of the $5p_{3/2}$ peak with respect to that of the $5p_{1/2}$ is probably due to the enhanced cross section of this state in the Auger-deexciation (AD) process. A similar ratio for the intensities of the $5p_{1/2}$ and $5p_{3/2}$ levels were found in MIES for Xe multilayers.[15]

SiO_2 is widely used as a support material in catalysis as well as a building block for various electronic devices.[16] Recently, very well-ordered SiO_2 thin films with a thickness of 0.7−0.8 nm have been prepared on a Mo(112) surface.[9,10] To obtain information on the wettability and uniformity of 0.7−0.8 nm thick SiO_2 films, MIES/UPS and MAX/PAX studies were carried out (Figure 2). The MAX spectrum of this SiO_2 thin film (Figure 2b) shows two narrow Xe 5p peaks, whose widths are comparable to those from the clean MgO(100) (Figure 1) and Mo(100) (Figure 3) surface, indicating that the SiO_2/Mo(112) surface is quite uniform, and the wettability of a SiO_2 thin film on Mo(112) is very high. In contrast to MAX, the Xe 5p features and the O(2P) peaks from SiO_2 overlap in the PAX spectrum (Figure 2a).

In Figure 3, the MIES spectra for Mo(100), MgO(100)/Mo(100), and SiO_2/Mo(112) collected with a Xe background pressure of 5×10^{-5} Torr at a sample temperature of 80 K are compared. The Xe $5p_{1/2}$ peak positions for SiO_2/Mo(112), Mo(100), and MgO(100)/Mo(100) are at 7.5, 8.0, and 9.5 eV, respectively. The work functions of SiO_2/Mo(112), Mo(100),

Figure 2. (a) UPS/PAX and (b) MIES/MAX spectra for SiO_2 thin film on Mo(112).
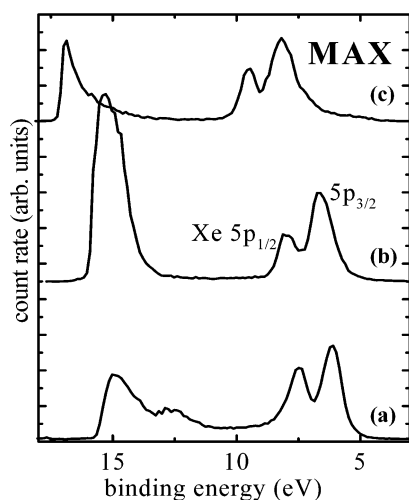
Figure 3. MIES spectra of adsorbed Xe (MAX) from (a) SiO$_2$/Mo(112), (b) Mo(100), and (c) MgO(100)/Mo(100).

and MgO(100)/Mo(100) estimated by the energy positions of the onset of the secondary electrons in the UPS spectra are 4.9, 4.4, and 2.9 eV, respectively;[17] thus, the sums of the work function and the 5p$_{1/2}$ energy positions for these three surfaces are constant, indicating that the Xe 5p$_{1/2}$ positions reflect the surface work function. It has been suggested that the 5p$_{1/2}$ binding energy of a Xe atom on the surface is pinned to the vacuum level of the surface such that the energy position of the Xe 5p$_{1/2}$ level with respect to the Fermi level can provide information about the surface work function,[2] in agreement with the results of Figure 3. The results in Figure 3 show that MAX can be used for wide band gap materials as well as metals, whereas the application of MIES is problematic for most transition metals due to high RI and AN yields.[3]

3.2. Identification of Defect Sites on Oxide Surfaces Using MAX. Defect sites on oxide surfaces can play a pivotal role in heterogeneous catalysis as reaction sites and nucleation sites of metal clusters, thus the identification of defect sites on oxide surfaces is important for obtaining a molecular-level understanding for various heterogeneous catalytic reactions. Using MAX, low and high defect MgO(100) surfaces can be characterized (Figure 4). The 300-K-grown MgO(100) film shows broader Xe 5p features in comparison to those of the 1150-K-annealed MgO(100) films, indicating that the surface of the 300-K-grown MgO(100) film is more heterogeneous. The MAX results are in line with the MIES and LEED results, since the 300-K-grown MgO film shows a broader O(2P) band, and a more diffuse LEED pattern, signatures for a higher defect density.[7]

The MAX spectrum of the high-defect MgO surface shows much less resolved features at lower binding energies with respect to the Xe 5p states of the low-defect surface. Assuming that the Xe 5p level is pinned to the vacuum level of the surface,[2] the local work function of the defect sites in the 300-K-grown MgO(100) films should be higher than that of the perfect MgO(100) surface. However, the work function of the 300-K-grown MgO(100) film determined by the onset of the secondary electrons in UPS is lower than that of the vacuum-annealed MgO(100) film, which does not agree with the MAX results. In contrast to the results for the low-defect surfaces (Figure 3), Figure 4 demonstrates that the Xe 5p levels in MAX do not always reflect the surface local work functions, and thus one should be careful in the determination for the local work functions of a heterogeneous surface using the Xe 5p energy positions, in particular for defect sites.
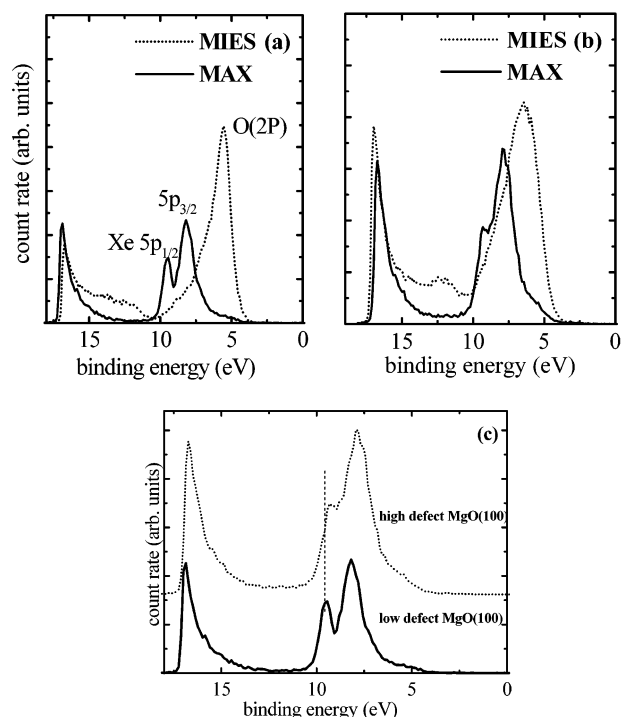

Figure 4. MIES and MIES of adsorbed Xe (MAX) for MgO surfaces with (a) low and (b) high defect densities. In (c), MAX spectra for both surfaces are compared. The high defect surface was prepared by deposition of Mg in an O$_2$ background of 1×10^{-7} Torr at room temperature. The low defective surface was prepared by deposition of Mg in a O$_2$ background of 1×10^{-7} Torr at 600 K, followed by multiple anneals at 1150 K. (Film thickness = approximately 15 monolayers.)
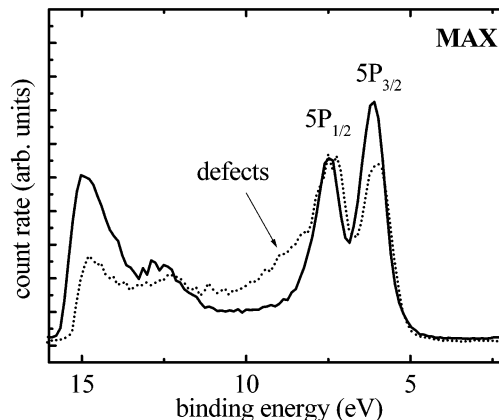

Figure 5. MAX for low and high-defect SiO$_2$ films on Mo(112).

In Figure 5, MAX spectra are shown for high- and low-defect SiO$_2$ surfaces prepared by annealing the 800-K-prepared film at 1050 and 1200 K, respectively. The defect sites on the high defect SiO$_2$ surface can be identified by a shoulder at higher binding energies with respect to the narrow doublet feature. For the high defect SiO$_2$ surface, no band gap state can be found in MIES, indicating that point defects such as oxygen vacancies and oxygen surplus sites are not present.[18] A broadening of the O(2P) band was found for the high-defect surface, resulting perhaps from an increased extended defect density, suggesting that the defect sites identified using MAX are extended defect sites such as steps and kinks.

3.3. Growth Mode of SiO$_2$ on Mo(112). Figure 6 shows MAX spectra acquired as a function of increased SiO$_2$ coverage on a Mo(112) surface. The lower MAX spectrum (Figure 6a) was collected from a Mo(112) surface, exposed to 300 langmuir
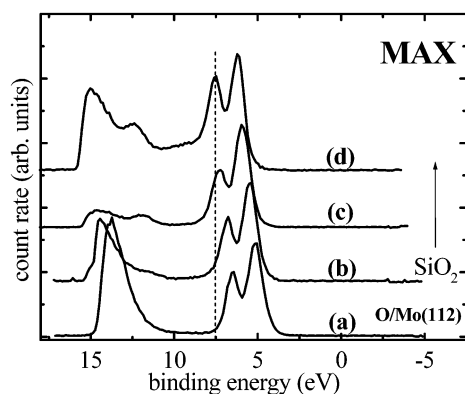
Surface Characterization Using MAX

J. Phys. Chem. B, Vol. 107, No. 2, 2003 **595**

Figure 6. MAX for various SiO_2 coverages on Mo(112). (a) clean Mo(112) exposed to 300 L of oxygen at 1200 K. (b) SiO_2 thickness = 0.2−0.3 nm. (c) SiO_2 thickness = 0.4−0.5 nm. (d) SiO_2 thickness = 0.7−0.8 nm.
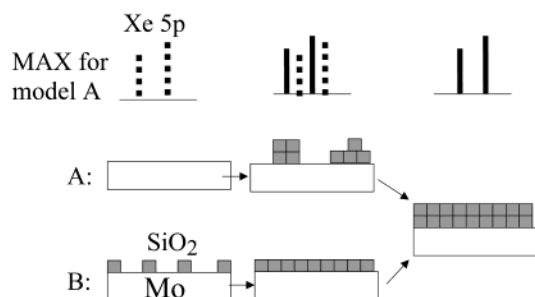

Figure 7. Different models for the growth of SiO_2 thin films, and the expected MAX results for model A. That the MAX spectra show gradual shifts without broadening of the Xe 5p peaks as a function of SiO_2 coverage indicates layer-by-layer growth of SiO_2 on Mo(112).

(L: 1×10^{-6} Torr s) of oxygen at 1200 K. The upper spectrum (Figure 6d) was acquired from an SiO_2 thin film with a thickness of 0.7−0.8 nm that showed a distinct $c(2 \times 2)$ LEED pattern.

The two most probable growth modes for SiO_2 on Mo(112) are shown schematically in Figure 7: large 3D SiO_2 island growth where the islands coalesce at higher SiO_2 coverages into a two-dimensional network (Figure 7A) and layer-by-layer growth (Figure 7B). The fact that the MAX spectra show gradual shifts without a change in the width of the Xe 5p peaks as a function of SiO_2 coverage suggests that SiO_2 grows in a layer-by-layer manner on Mo(112). Three-dimensional island formation, in contrast, should lead to a broadening of the MAX peaks or the appearance of additional features in the MAX peaks at the initial stage of the SiO_2 growth (Figure 7A).

3.4. Decomposition of MgO Films upon Annealing. The MAX spectra for the MgO(100)/Mo(100) films after annealing at various temperatures are shown in Figure 8. After annealing at 1320 K, no change of the MAX spectrum is apparent, however, annealing at 1400 K lowers the intensities of the MgO(100)/Mo(100) peaks, whereas a new doublet feature appears at lower binding energies. These results show that decomposition of MgO(100) films takes place upon annealing, exposing some of the Mo(100) surface. The energy positions of the Xe 5p peaks from the uncovered Mo(100) surface in Figure 8 are lower by 0.4 eV with respect to those of the clean Mo(100) surface in Figure 3. Therefore, it is not likely that clean Mo(100) is exposed after annealing MgO(100)/Mo(100) at 1400 K, but rather MgO islands and oxygen-covered Mo(100) (or Mo oxide) are present. In the MIES/UPS spectra, a decrease in intensity of MgO features and an increase of the Mo features are observed after annealing at >1400 K, in line with the MAX/PAX results.[19] These results are consistent with previous TPD
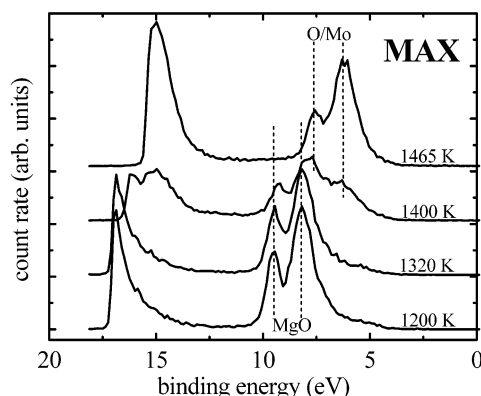

Figure 8. MIES of adsorbed Xe (MAX) spectra for MgO/Mo(100) acquired after annealing at various temperatures.

studies that showed thermal decomposition of MgO within the temperature range of 1300−1460 K.[20] From the absolute intensities of the Xe 5p peaks in MAX, it is concluded that about 70% of the Mo surface is covered by MgO islands after annealing at 1400 K, implying that MAX can be used for the quantitative analysis of nonuniform oxide surfaces.

4. Conclusions

It is shown that for MgO and SiO_2, UPS spectra of adsorbed Xe (PAX) provides rather ambiguous data because of the overlap of the Xe-induced features with those of the substrate. However, with MIES of adsorbed Xe (MAX), only features from the Xe monolayers are detected, i.e., the substrate signals are completely quenched. Several examples are given illustrating the usefulness of MAX for the characterization of various surface morphologies. For example, the high crystallinity and wettability of SiO_2 and MgO thin films on Mo(112) and Mo(100) have been confirmed using MAX. Defect sites on MgO and SiO_2 films, which can play a pivotal role in model catalysts, can be identified using MAX. These results show that MAX can be used to quantitatively characterize solid surfaces, broadening the applicability of MIES.

References and Notes

(1) Jablonski, A.; Wandelt, K. *Surf. Interface Anal.* **1991**, *7*, 611.

(2) Wandelt, K. Appl. *Surf. Sci.* **1997**, *111*, 1.

(3) Harada, Y.; Masuda, S.; Ozaki, H. *Chem. Rev.* **1997**, *97*, 1897.

(4) Kolmakov, A.; Stultz, J.; Goodman, D. W. *J. Chem. Phys.* **2000**, *113*, 7564.

(5) Mausfriedrichs, W.; Dieckhoff, S.; Kempter, V. *Surf. Sci.* **1991**, *249*, 149.

(6) Mausfriedrichs, W.; Wehrhahn, M.; Dieckhoff, S.; Kempter, V. *Surf. Sci.* **1990**, *237*, 257.

(7) Kim, Y. D.; Stultz, J.; Goodman, D. W. *J. Phys. Chem. B* **2002**, *106*, 1515.

(8) Kim, Y. D.; Stultz, J.; Goodman, D. W. *Surf. Sci.* **2002**, *506*, 228.

(9) Schroeder, T.; Adelt, M.; Richter, B.; Naschitzki, M.; Baumer, M.; Freund, H.-J. *Surf. Rev. Lett.* **2002**, *7*, 7.

(10) Schroeder, T.; Hammoudeh, A.; Pykavy, M.; Magg, N.; Adelt, M.; Baumer, M.; Freund, H. J. *Solid-State Electron.* **2001**, *45*, 1471.

(11) Hulse, J.; Kuppers, J.; Wandelt, K.; Ertl G. *Appl. Surf. Sci.* **1980**, *6*, 453.

(12) Scheffler, M.; Horn, K.; Bradshaw, A. M.; Kambe, K. *Surf. Sci.* **1979**, *80*, 69.

(13) Dolle, P.; Markert, K.; Heichler, W.; Armstrong, N. R.; Wandelt, K.; Kim, K. S.; Fiato, R. A. *J. Vac. Sci. Technol. A* **1986**, *4*, 1465.

(14) Johnson, M. A.; Stefanovich, E. V.; Truong, T. N.; Gunster, J.; Goodman, D. W. *J. Phys. Chem. B* **1999**, *103*, 3391.

(15) Oro, D. M.; Soletsky, P. A.; Zhang, X.; Dunning, F. B.; Walters, G. K. *Phys. Rev. A* **1994**, *49*, 4703.

(16) Pacchioni, G.; Skuja, L.; Griscom, D. L. *Defects in SiO$_2$ and related dielectrics: Science and Technology;* NATO Science Series 2002.

(17) Kim, Y. D.; Wei, T.; Stultz, J.; Goodman, D. W. Unpublished results. 2002.

(18) Pacchioni, G.; Ierano, G. *Phys. Rev. B* **1998**, *57*, 818.

(19) Kim, Y. D.; Stultz, J.; Goodman, D. W. Unpublished results. 2002.

(20) Wu, M. C.; Truong, C. M.; Goodman, D. W. *Phys. Rev. B* **1992**, *46*, 12688.